Assessment of building damages and risk under extreme flood scenarios in Shanghai

Jiachang Tu[1,2], Jiahong Wen[1*], Liang Emlyn Yang[2*], Andrea Reimuth[2], Stephen S. Young[3], Min Zhang[1], Luyang Wang[1], Matthias Garschagen[2]

5   [1]School of Environmental and Geographical Science, Shanghai Normal University, 200234 Shanghai, China
[2]Department of Geography, Ludwig Maximilian University of Munich (LMU), 80333 Munich, Germany
[3]Geography and Sustainability Department, Salem State University, 01970 Salem, USA

Correspondence to: J. Wen (jhwen@shnu.edu.cn), L.E. Yang (emlyn.yang@lmu.de)

Abstract. This article presents a flood risk assessment in Shanghai, doing so will provide an indication of what buildings
10 (including residential, commercial, office, and industrial buildings) will be exposed to flooding and its damage. Specifically, the assessment provides risk assessment that buildings may face after construction. To achieve the flood risk assessment on Webuildings, we developed an integrated flood model and collect data on buildings' shape and storey, land use, and construction cost in different types in Shanghai. The extreme compound flood scenarios and buildings' metadata were aggregated using a risk analysis chain, according to the damages for different flood scenarios, the average annual loss (AAL)
15 can be calculated and is referred to as building flood risk. The AAL of residential, commercial, office, and industrial buildings are 12.3, 2.5, 3.7, and 3.4 million USD, respectively. Among the 15 (non-island) districts in Shanghai, Pudong has the highest AAL. The risk analysis chain developed in this study can be reproducible to other megacities. The result provides a clear enough future for building flood risk which links directly to disaster risk management, implies the extent of flood risk in building types, districts, and communitiessub-districts to the Shanghai Master plan, references result to future climate change
20 scenario framework, information for scenario-based decision making and cost-benefit analysis for extreme flood risk management in Shanghai. We also discussed different potential adaptation options for flood risk management.

1 Introduction

Risk, in the context of climate change impacts as outlined in the latest IPCC report, refers to result from dynamic interactions between climate-related hazards with the exposure and vulnerability of the affected human or ecological system to the hazards
25 (IPCC, 2022). To be more specifically, Ccoastal cities that have historically suffered from and will continue to be heavily impacted by the increasing risks and effects of rising floods major flood impacts, such as Dhaka, Guangzhou, Miami, Mumbai, New Orleans, and New York, are heavily affected by future rising flood risks to their population and assets (Woetzel et al., 2020a; Nguyen et al., 2021; Chan et al., 2021). By 2050, over 570 low-lying coastal cities and their 800 million inhabitants will face risks from the impacts of floods and rising sea levels, causing economic losses of up to 1 trillion USD (C40Cities,
30 2018). Although many coastal cities are facing increasing flood risks (Liang et al., 2017), some will be more seriously affected than others due to local climate change effectsimpacts, high exposure, or limited adaptation capacities. One of the hotspots, which is facing high flood risks already today, is Shanghai.

Compared to other coastal cities, like Dhaka, Manila, and Rotterdam, Shanghai is the most vulnerable city to flooding (Balica et al., 2012). Coupled with factors of human (population exposure and property exposure) and environment (low-lying land,
35 land subsidence problems, the threat of sea-level rise, frequent typhoons, and extreme precipitation) relationships, Shanghai is ranked as one of the top 20 cities for flooding in the world (Hallegatte et al., 2013; Wu et al., 2019). As an answer to this obstacle, Shanghai, the most developed financial centre in China, should apply a flood risk assessment to simulate multi flooding scenarios with integrated flood model, and drive damage based on the damages of tangible economic sectors, such as architectural structures.

40   For Shanghai, it is necessary to consider extreme flood events, which caused dike overtopping and hinterland storage, in the flood models. Since the 1950s, hard measures, like seawalls (along the Yangtze River Estuary and Hangzhou Bay) and levees (along the Huangpu River), were constructed in Shanghai (Zhou et al., 2017). However, the seawalls and levees can be easily destroyed due to the poor structures and lower standards during the various stages of construction (Zhou et al., 2017). Only 23 % of seawalls can withstand a 200-year flooding scenario; 58 % of seawalls can withstand a 100-year flooding scenario while

45   the rest of seawalls withstand less than a 100-year flooding scenario (Wang et al., 2012). The present protection level of the levees along the Huangpu River for the lowest sections is around 1/50-year flooding scenario (Ke et al., 2018). Meanwhile, the historical crest heights in the Huangpu River reveals a significant growing trend from 1950 to 2000, with the existing levees failing several times and leading to extreme damage (Ke et al., 2018), posing a greater threat to Shanghai. Overall, to protect Shanghai from a future failure of floodwalls and levees, extreme flood scenarios, and their consequences should be the

50   taken as the first step of an integrative risk assessment.

       Reviewing the current literature shows that various flood modelling techniques and flood scenarios have been developed for estimating flood risks in Shanghai. Coastal floods (storm surge from Shanghai's coast) and fluvial floods (river flood from the Huangpu River) are the two types of floods which have been the focus for Shanghai. Coastal flood scenarios from the Shanghai coast have been forecasted for 2030 and 2050 by Yin et al. (2011), as well as 2030, 2050, and 2100 by Wang et al. (2012).

55   These scenarios have examined the effects of factors like sea-level rise and storm surge (Yin et al., 2011), or integrated effects like sea-level rise, land subsidence, and storm surge (Wang et al., 2012). In addition to examining the effects on the Shanghai coast, Yin et al. (2013) looked at how sea-level rise and subsidence combined with storm tide-induced river flooding in the Huangpu River floodplain in 2030 and 2050. Yin et al. (2015) used a 2D hydrodynamic model to estimate 1/10, 1/100, and 1/1000-year flood scenarios in the Huangpu River floodplain in Shanghai based on historical floodplain data. The flood

60   scenarios produced in most existing studies tended to focus on the possible future flood scenario changes rather than extreme events, e.g., the concern floods over a 1000-year return period (Yin et al., 2011; Wang et al., 2012; Yin et al., 2013, Yin et al., 2015). At the same time, according to the IPCC report, extreme seal level rise events are projected from once per century to once per year (IPCC, 2019) which could increase the frequency of extreme flood events for coastal cities, such as Shanghai, in the future. Therefore, Shanghai demands multiple extreme compound flood scenarios that combine fluvial and coastal
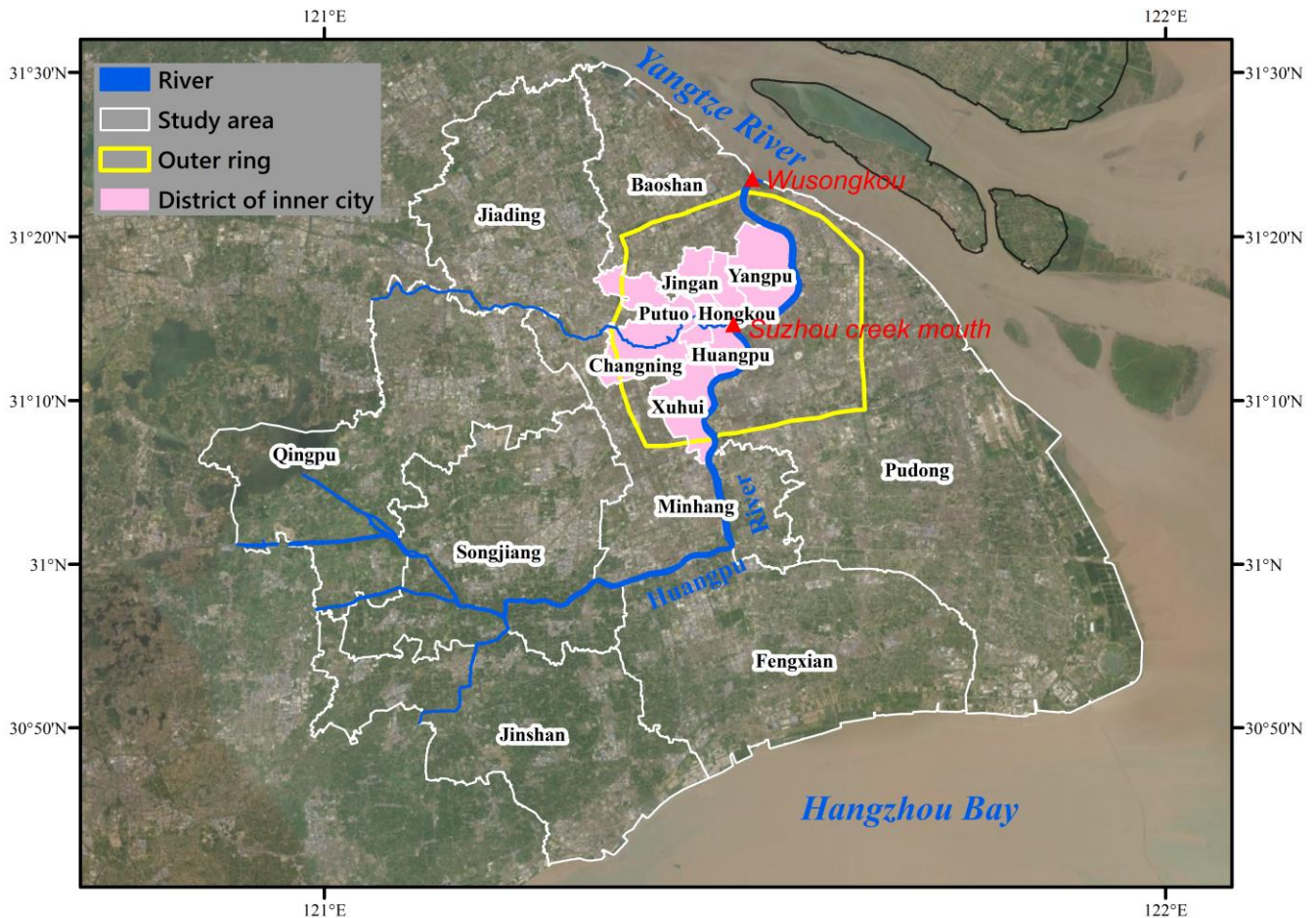
65   flooding.

       The previous studies are dedicated to simulating floods or flooding in Shanghai instead of focusing on the overall risks. The consequences of flooding (i.e., construction damage), however, should be taken into consideration. Flood damage to buildings is noticeably a large part of the total flood losses in cities (Chmutina et al., 2014; Park and Won, 2019), in addition to the often devastating human costs (Woetzel et al., 2020a). In 1997, Typhoon Winnie caused large-scale flooding in Shanghai and

70   affected more than 5000 households (Du et al., 2020). In 2008, floods damaged 160 streets and 13,000 residential buildings in Shanghai. Therefore, local communities and governmental departments are increasingly calling for holistic analyses of possible building damage under extreme flood scenarios in order to accurately understand and assess potential flood impacts (Kelman and Spence, 2004). To estimate building stocks and the values at risk under a 1/1000-year extreme flood scenario, Wu et al. (2019) integrated census-level building floor-area data and geo-coded building asset value data. Shan et al. (2019) further

75   assessed the flood losses of residential buildings and household properties in Shanghai based on a stage-damage function, building footprint, and housing prices. Mostly, deeper investigations into the uncertainties (e.g., asset values, damage rate, and flood process) with reliance on flood risks and damages of buildings (e.g., residential, commercial, office, and industrial) are also urgently needed in order to better support decision making which enhances the overall flood resiliency of the city.

       To address these questions, we adopted the very extreme flood scenarios with return periods of 1/200, 1/500, 1/1000, and

80   1/5000-year representing a low probability-high impact scenario. The four extreme flood scenarios are assumed as combined effects of several flood-triggering factors, such as typhoon-induced storm surge, precipitation, fluvial flooding in combination with a high astronomical tide, to reflect low probability-high impact flood situations in Shanghai. The objective of this paper

is to assess flood risk and its pattern of residential, commercial, office, and industrial buildings under extreme flood scenarios in Shanghai. To achieve this objective, we modelled building inundations at four extreme flood scenarios with return periods

85　of 1/200, 1/500, 1/1000, and 1/5000-year, respectively. Combining the inundation maps with the stage-damage functions, the study evaluated and identified the spatial distribution of damages for the specific types of buildings in Shanghai. Section 2 of the paper introduces, Shanghai, the study area. Section 3 describe the details of the materials and methods, and section 4 presents the data analysis and major results of the study. Section 5 discusses future flood scenarios and proper adaptation strategies for building a flood-resilient Shanghai. Final conclusions are described in section 6.

90　**2. Study area**

Shanghai is the biggest coastal city in China in terms of population (24.3 million in 2019) and is the major trading and financial hub of China. The city has an area of 6340.5 km^2 that lies in the Yangtze River Delta along the northern edge of Hangzhou Bay (Figure 1). Shanghai is prone to flooding because of its flat low-lying terrain, as well as its location on the path of frequent typhoons from the northwest Pacific (Balica et al., 2012). Moreover, the city experienced an average land subsidence of 1.97

95　meters from 1921 to 2007 and the trend is continuing (Gong and Yang, 2008) additionally driving flood risks (Quan, 2014). In addition, according to the Shanghai Statistical Yearbook, 29.1 billion USD (183.4 billion CNY) is invested in architectural construction in Shanghai which includes residential buildings (15.3 billion USD), office buildings (4 billion USD), commercial buildings (4 billion USD) and others (5.8 billion USD) in 2019 (SMBS, 2020).

100　Figure 1. Satellite image-based map of the study area (Shanghai's 15 districts, excluding the city's islands) (The satellite image background is from Esri).

3 Materials and methods

In our study, the flood risks in Shanghai are estimated using three different steps (Figure 2): first, extreme flood scenarios with a return period of 1/200, 1/500, 1/1000, and 1/5000-years are simulated by an integrated flood model. This was done in a previous work by Wang et al., (2019). Our study builds upon these results and estimates the damages based on the obtained flood hazard scenarios. Finally, the overall flood risk and its spatial pattern for buildings in Shanghai, described as the estimated average annual loss (AAL). More details of the assessment are introduced in the following sections 3.1 to 3.3.
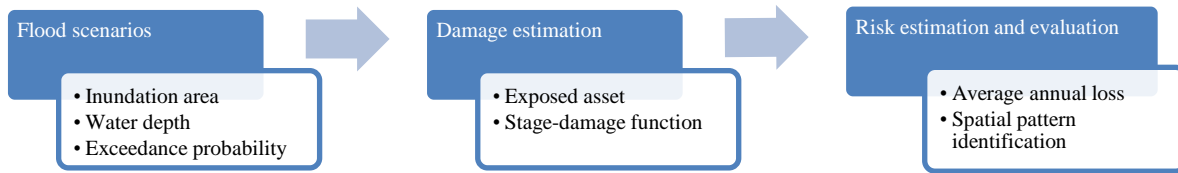

Figure 2. Risk analysis chain

3.1 Flood scenarios

The flood scenarios build on the results of Wang et al. (2019), who used an integrated flood model to simulate compound flooding in Shanghai that included fluvial and coastal flooding. Four scenarios with return periods of 200, 500, 1000, and 5000 years were simulated considering atmospheric conditions, oceanic/coastal environments, and river discharge.

For this purpose, the integrated model has applied and coupled several models in three stages: in the first stage, the Fujita model provides the atmospheric conditions on the north-western Pacific Ocean (from 100 - 180 °E for longitude, 0 - 60 °N for latitude). The Fujita model computed and simulated Typhoon Winnie's wind direction, speed, press, and boundary layer. Typhoon Winnie was a typical turning track typhoon, bringing the highest recorded water level of 5.72 meters in Shanghai since 1900 (Dong et al., 2022). Wind data from Typhoon Winnie were required from European Centre for Medium-Range Weather Forecasts (ECMWF). Then the atmospheric conditions integrated with the TELEMAC model provide the oceanic/coastal environment on the Yangtze River Delta (from 120 – 124.5 °E for longitude, 28 - 34 °N for latitude). The TELEMAC model simulates the hydrodynamic and morphodynamical process in oceanic/coastal environments including shallow water horizontal flows and waves from the Pacific Ocean (Hashemi et al., 2015). The first two stages prepare parametric for the coastal flooding from Shanghai's coast. In the last stage, the atmospheric and the oceanic/coastal condition have been integrated with the MIKE model which simulates the river discharge in the study area. Rainfall and river discharge measurement data from Typhoon Winnie were implemented in the MIKE model. The MIKE Model is applicable for the simulation of hydraulic for fluvial flooding from the Huangpu River (MIKE, 2017).

This model offers Shanghai extreme compound flood scenarios with inundation area and depth at a resolution of 60 m. These extreme compound flood scenarios are being shown for the first time in Shanghai with 200, 500, 1000, and 5000 years return periods.

3.2 Damage estimation

3.2.1 Asset value of buildings

From Baidu Map (Baidu Maps, ~~2017~~2018) the data for Shanghai's buildings were acquired using a python-based web crawler, and then processed with ArcGIS software. Baidu Maps provide various map services, such as satellite images, street maps, and route planners in China. The shapefile data for Shanghai's buildings include the information of building type, building ground-based area, height, and the number of floors for each building. The data of Shanghai's buildings are combined with land use data to further cluster the buildings into four different types including: residential, commercial, office, and industrial. The land use data of 2013 from the Shanghai Planning and Land Bureau was depicted hierarchically into 3 sectors, 15 subcategories, and 73 subclasses of land use types using ArcGIS 10.6.1. The reclassification of the land use was conducted

4

according to the National Standard of China "GB/T 2010-2017" (CSP, 2017) and covers residential area, commercial area,

140 office area, and industrial area. The land use type of residential area covers apartment, mixed apartment, rural housing, and

empty housing. Office areas include land for medical care and health, charity, education, culture, government, research, market, and insurance.

The cost data of building construction used in this study are derived from the 2019 annual report provided by the consulting company Arcadis in Shanghai. The data set depicts five different building types (domestic, office/commercial, hotels,

145 industrial, and other), which are further divided into 19 subsectors (Arcadis, 2020). Due to the lack of details about the architectural construction, the construction costs of various buildings are equally weighted (Table 1). The average construction cost is derived from the average number of the construction cost in the four different building types.

Table 1. Common construction costs of various buildings in Shanghai.

	Building Type	Construction Cost (USD/m^2)	Average Construction Cost (USD/m^2)
Residential	Apartments, high rise, average standard	668-740	874
	Apartments, high rise, high end	1554-1697	
	Terraced houses, average standard	446-477	
	Detached houses, high end	666-740	
Commercial	Retail malls, high end	1228-1585	1407
Office	Medium/high rise offices, average standard	868-1156	1157
	High rise offices, prestige quality	1158-1445	
Industrial	Industrial units, shell only (Conventional single story framed units)	432-540	486

150 Different methods exist in the evaluation of building values. According to the Chinese National Standard (GB/T 50291-2015) and previous studies, there are four main approaches to evaluate the asset value of buildings: method of the sales comparison, method of the income capitalization, method of the construction cost, and method of the hypothetical development (CSP, 2015). The application of different methods depends on the specific study aims and the availability of building-specific data. Sale comparison is often used when the evaluation of a similar type of building is available, whereas the income capitalization

155 is suitable for buildings that yield profits like rents. If a building is newly constructed or (to be) reconstructed after damage, method of construction cost would be suitable for the evaluation. The method of hypothetical development is applicable to the evaluation of real estate with investment development or redevelopment potentials. Since the present study aims to assess flood damages on buildings, the construction cost method is used with consideration of the building surface area. Then, the asset value of one building can be approximated by the following function:

160
$$W_n = S_n \times P_n \qquad (1)$$

Where W_n (USD) is the asset value for one building which belongs to the building type n, S_n is the surface area of building n, P_n is the average construction cost (USD/m^2) for the specific type of building n. The surface area is the whole construction area (including wall area and floor area).

Table 2. Examples of building asset value for the four selected building types.

Building id	Building type n	Surface area (m^2)	Average construction cost (USD/m^2)	Asset Value (USD)
1	Residential building	1662	874	1452588
2	Commercial building	1347	1407	1895229
3	Office building	776	1157	897832
4	Industrial building	2463	486	1197018

165 **3.2.2 Evaluation of building damages in flood**

The relationship between flood inundation depth and flood damages of a building or other property is depicted by a stage-damage function (Garrote et al., 2016; Mcgrath et al., 2019). In this study, the stage-damage functions are adapted from existing

studies on the relationship of various building damages rate with water-level depth in Shanghai (Ke, 2014). Based on actual building damage data from past flood hazard events and previous empirical stage-damage functions in Shanghai (Yu et al., 2012; Wang, 2001), Ke (2014) developed updated stage-damage functions to specific buildings in Shanghai. The stage-damage function is used to evaluate the damage values of residential, commercial, office, and industrial buildings with the probability of 1/200, 1/500, 1/1000, and 1/5000-years extreme flood scenarios, respectively. As shown in Table 3, the stage-damage functions represent the average damage in dependency of the inundation depth for the four adopted building types. If the building is flooded at depth of more than 3 meters, we assume that the exposed area covers two floors instead of one.

Table 3. Selected stage-damage functions for the study area (Adapted from Ke (2014)).

Inundation depth (m)	Residential buildings	Commercial buildings	Office buildings	Industrial buildings
<0.5	0.03	0.05	0.03	0.03
0.5-1.0	0.06	0.09	0.07	0.08
1.0-1.5	0.09	0.13	0.12	0.11
1.5-2.0	0.12	0.18	0.14	0.15
2.0-2.5	0.16	0.22	0.18	0.19
2.5-3.0	0.19	0.27	0.20	0.22
>3.0	0.22	0.31	0.25	0.25

The damage values of one building can be expressed by the following function:

$$D_n = E_n \times P_n \times T_n \tag{2}$$

Where D_n represents building damage for building type n, E_n represents the exposed area of buildings for building type n, P_n is the construction cost (USD/m^2) for the specific type of building n, T_n represents the damage proportion from stage-damage function for building n under different water-level depths.

Table 4. Examples of damage values for the four building types at an inundation level of 0.5-1 m.

Building id	Building type n	Exposed area (m^2)	Average construction cost (USD/m^2)	Damage proportion	Building damage (USD)
1	Residential building	123	874	0.06	6450
2	Commercial building	341	1407	0.09	43180
3	Office building	539	1157	0.07	43653
4	Industrial building	29	486	0.08	1127

3.3 Risk Determination and Evaluation

When expressing a city-scale flood damage for different flood scenarios, we use the already well established economic AAL (Hallegatte et al., 2013). The AAL is the sum of the probabilities of floods for each return period, while considering the approximate areas under the associated risk curve (Ward et al., 2011). In the present study, we considered only the damage value of buildings as a major part of the AAL. Particularly, the AAL represents the integrative building damage for all types of buildings in all the considered flood scenarios in Shanghai. Hence, we get the AAL values for different exceedance probabilities (extreme flood scenarios) as the sum of:

$$\text{AAL} = \int x \, f(x) dx \tag{3}$$

Where x is the return period of the flood scenario, and $f(x)$ is the damage value of a single type of building.

The AAL of all sub-districts and their neighbours were compared with the AAL by Getis-Ord Gi* in ArcMap 10.6. The Getis-Ord Gi*, also known as the hot spot analysis, measures the strength of spatial autocorrelation and tests the assumption of independence between surrounded features (Manepalli et al., 2011). According to the Getis-Ord Gi*, a feature with a positive value and intense clustering of high values, the feature corresponds to hot spot clusters, a feature with a negative value and intense clustering of low values, the feature corresponds to cold spot clusters. The results contain a significant range of high

values (hot spots) and low values (cold spots). In our study, hot spots mean the flood risk of a sub-district has a high AAL value and is surrounded by other sub-districts with high values, and has a higher risk for extreme flooding. Cold spots indicate an opposite situation.

4 Results

4.1 Mapping the flood scenarios

The four extreme flood scenarios present the comparison of the spatial distribution of inundation areas (Figure 3). The inundation areas increase generally, but non-linearly, along with increasing return periods. As shown in figure 3, the inundation areas mainly concentrate in regions around the Wusongkou (the mouth of Huangpu River), the Suzhou creek mouth (central Shanghai), the Songjiang-Qingpu low-lying area, and the north bank of Hangzhou Bay. The inundation areas expand to inland areas from the coastal region and the rivers as the flood scenario becomes more extreme. For the 1/200-year flood scenario, 9 % (488 km^2) of Shanghai is flooded, mainly along the north bank of Hangzhou Bay. The flooded area of Shanghai increased to 16 % (868 km^2) and 24 % (1302 km^2) in the 1/500-year and 1/1000-year flood scenarios, respectively. The flooded area extended significantly to 49 % (2659 km^2) of Shanghai in the 1/5000-year flood scenario. More specifically in this exceptionally extreme scenario, 32 % of the city would be flooded with a water depth of 0-0.5 m, 11 % with a 0.5-1.0 m depth of water, and 5 % with a water depth of more than 1m (Figure 3).
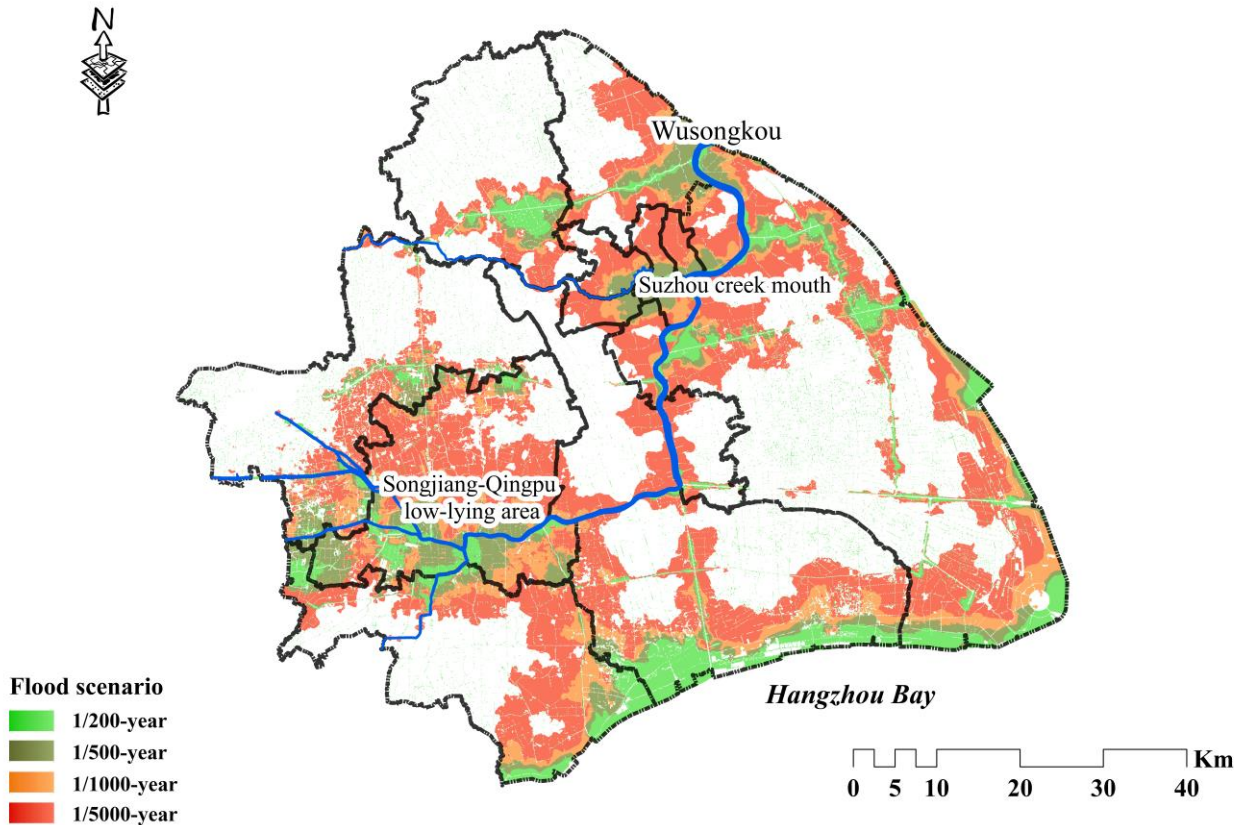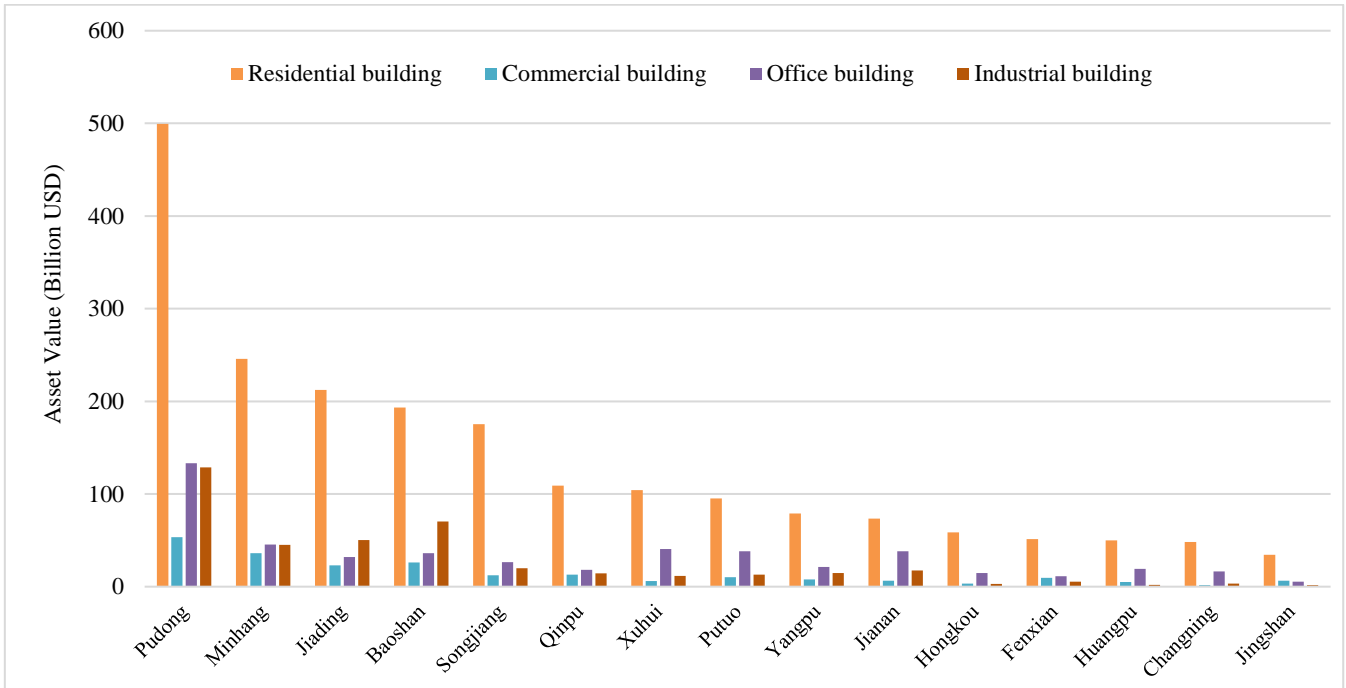

Figure 3. Inundation areas for the four flood return periods in Shanghai (excluding the area of islands).

4.2 Estimating the building damage

This study identified the building surface area of each type of building in 2017, which amounts to 2323 km^2, 157 km^2, 430 km^2, and 824 km^2 respectively for the residential, commercial, office, and industrial buildings. This is a conservative estimation as the actual present value of the buildings are certainly higher due to new developments in recent years. Every single building's asset value has been computed using equation (1), allowing us to obtain the number of building asset values in residential,

commercial, office, and industrial buildings. According to equation (1), the building asset values in Shanghai are 2030, 221, 497, and 401 billion USD considering the Average Construction Cost (see Table 1) of each building types in 2019. The relative

220 numbers show that residential buildings have the highest asset value, followed by office, industrial, and commercial buildings. While comparing the building asset values in the 15 districts, the Pudong district has the highest asset value (Figure 4) as it is the largest district in Shanghai. Our estimate for the building assets underpins the importance to quantify the value of architectural construction in Shanghai, along with the value of damaged architectural construction.

225 Figure 4. The building asset values in the 15 districts of Shanghai.

The quantitative assessment provides maps of flood damages to different buildings under the four extreme scenarios (Table 5). The total building damages in the 1/5000-year flood scenario is 15 billion USD, which is more than 13 times the 1/200-year flood scenario (1.18 billion USD). Again, residential buildings are the most damaged in all four scenarios with a damage value of up to 8.2 billion USD in the 1/5000-year scenario. Damages of industrial buildings, office buildings, and commercial

230 buildings would reach 2.6, 2.8, and 1.6 billion USD respectively under the 1/5000-year flood scenarios.

Table 5. Damage statistics for residential, commercial, office and industrial buildings exposed to extreme flooding under the four return period scenarios in Shanghai's 15 (non-island) districts (Unit: Billion USD).

Asset Damages District	Return Periods			
	1/5000	1/1000	1/500	1/200
Jiading	0.71	0.37	0.26	0.17
Fengxian	0.45	0.23	0.17	0.14
Baoshan	2.06	0.89	0.50	0.09
Xuhui	0.88	0.25	0.14	0.02
Putuo	1.05	0.44	0.22	0.01
Yangpu	0.94	0.28	0.11	0.01
Songjiang	1.11	0.29	0.10	0.03
Pudong	4.00	1.44	0.94	0.50
Hongkou	0.65	0.20	0.10	0.00
Jinshan	0.31	0.13	0.08	0.04
Changning	0.66	0.34	0.18	0.00
Minhang	0.47	0.04	0.02	0.02
Qingpu	0.17	0.09	0.05	0.03
Jinan	1.01	0.51	0.38	0.08
Huangpu	0.78	0.44	0.22	0.05

	Total	15.26	5.95	3.45	1.18

The damage analysis of different districts shows that Pudong has the highest overall damage in all scenarios (Table 5).
However, the rankings of the proportion of damages are different. For the 1/200-year scenario, Fengxian has the highest
proportion of asset damages. Jingan has the highest damage proportion in the 1/500-year scenario. While for the 1/1000 and
1/5000-year scenarios, Huangpu is the district with highest proportion of asset damages (Figure 5).
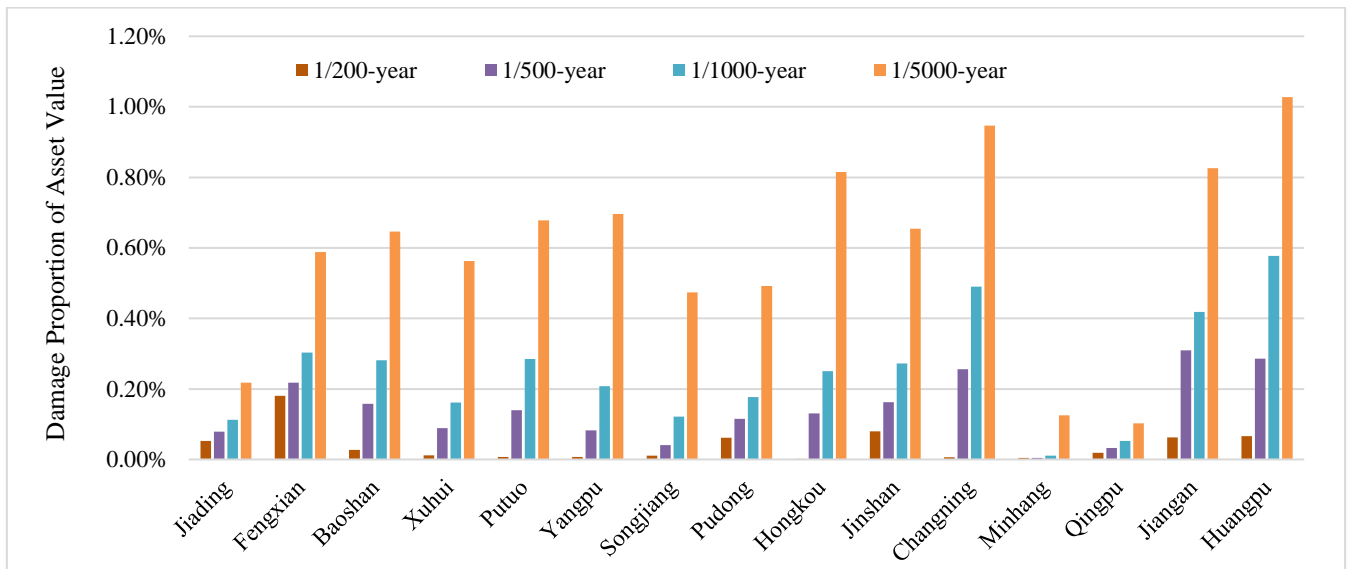

Figure 5. Damage percentages of residential, commercial, office and industrial buildings to extreme flooding under the four
return period scenarios in each district.

In terms of damage due to water depths in different flood scenarios, water depths of 0-0.5 m caused 83 % of building damage
in the 1/200-year flood scenario. Under 1/500, 1/1000, and 1/5000-year flood scenarios, the proportions are 67 %, 55 %, and
45 %, respectively, with deeper water depths causing more damage. For instance, 33 % of buildings are damaged in water
depths of 0.5-1 m under the 1/5000-year flood scenario, and 18 % of the damages occur in water depths 1-1.5 m (Figure 6).
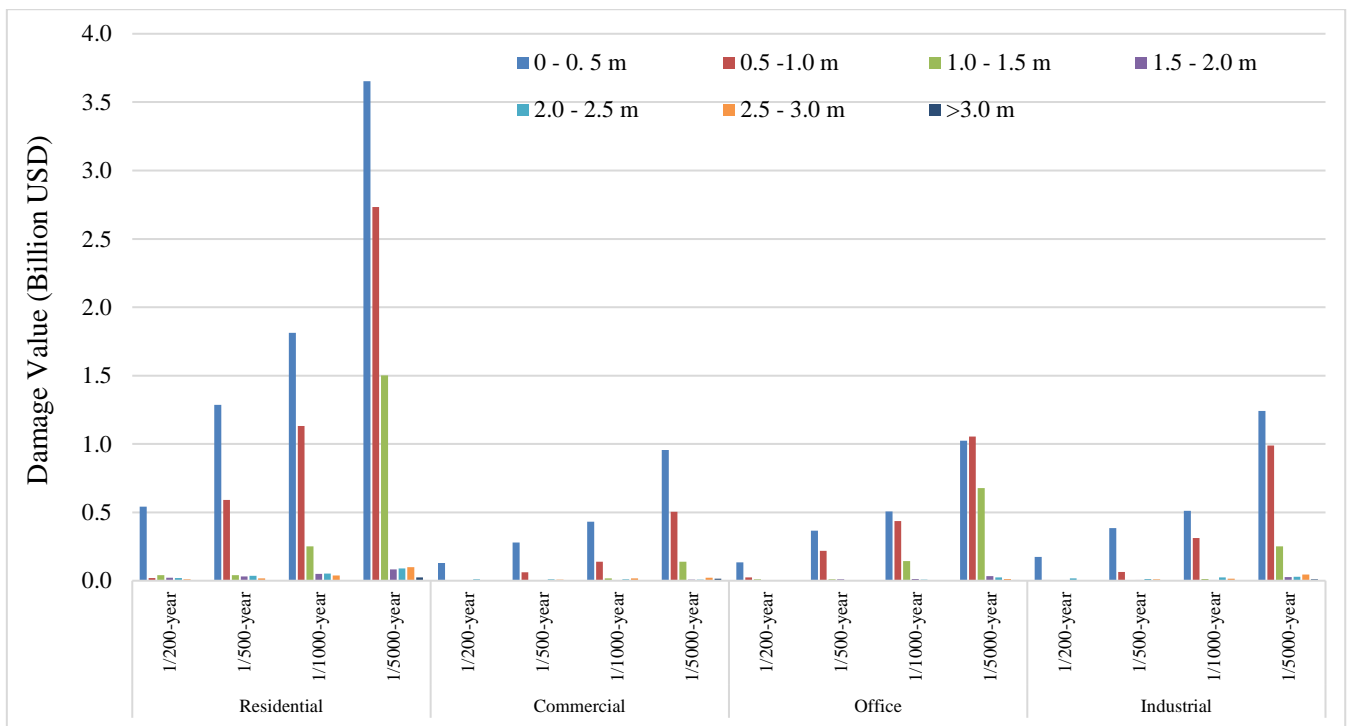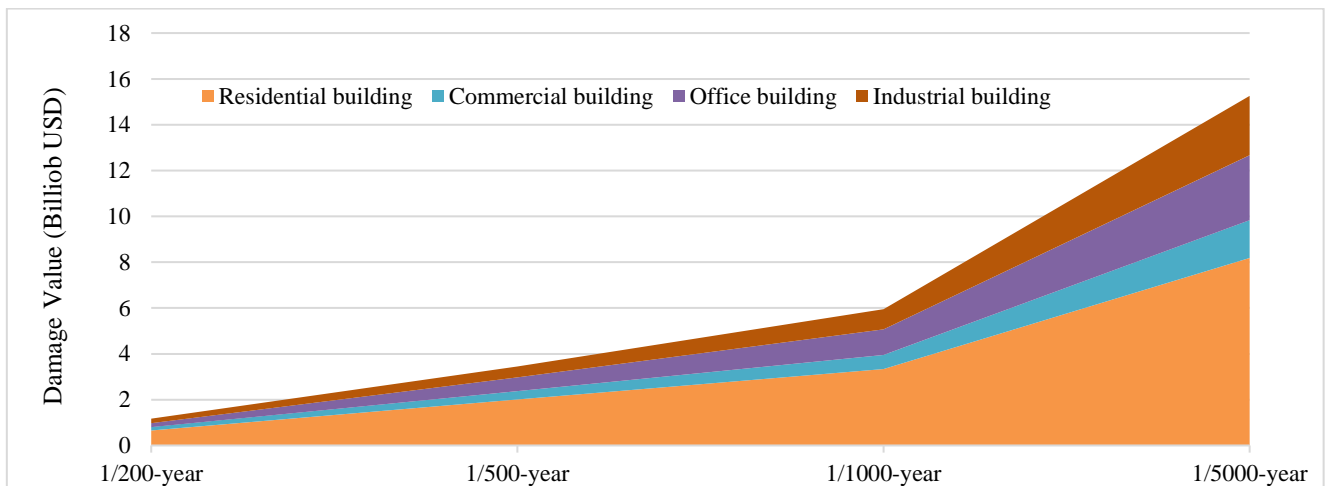

Figure 6. The damage asset for different water depths.

4.3 Risk estimates of buildings and its pattern

By integrating the extreme flood scenarios and associated building damages for the four types of buildings, we plotted four average annual probability-damage curves (Figure 7). The AALs of residential, commercial, office, and industrial buildings are 12.3, 2.5, 3.7, and 3.4 million dollars, respectively. It shows that residential buildings would suffer the highest risk value among the four types of buildings.

By using the Getis-Ord Gi* statistic tool in ArcMap 10.6, the results reveal the distribution of high and low building risks for different types of buildings at the ~~community~~ sub-district level in Shanghai (Figure 8). Apparently, the distribution of hot spots and cold spots for different types of buildings are quite different. For residential buildings, there are six hot spot areas and five cold spot areas. Most of the hot spot areas concentrate in the city center, except for one along the north coast of Hangzhou Bay. Further analysis of the commercial buildings indicates a significant hot spot south of the Suzhou Creek Mouth. Figure 8 shows five hot spot areas and two cold spot areas for office buildings with three hot spots located in coastal areas. Four hot spots of industrial buildings concentrate mainly in the north, while the city center is the main cold spot area because there are few industrial buildings located there.

Overall, the city center is the hot spot area of flood risk for the residential, commercial, and office buildings (Figure 8a, 8b and 8c). But in contrast, the city center is the cold spot area for the industrial buildings (Figure 8d). Wusongkou is affected by flooding with an expanding inundation area under increasing return-periods. One reason for this is that the density of buildings in Wusongkou is higher than in other areas.

Figure 7. Probability-damage curve of extreme flooding for residential, commercial, office, and industrial buildings.
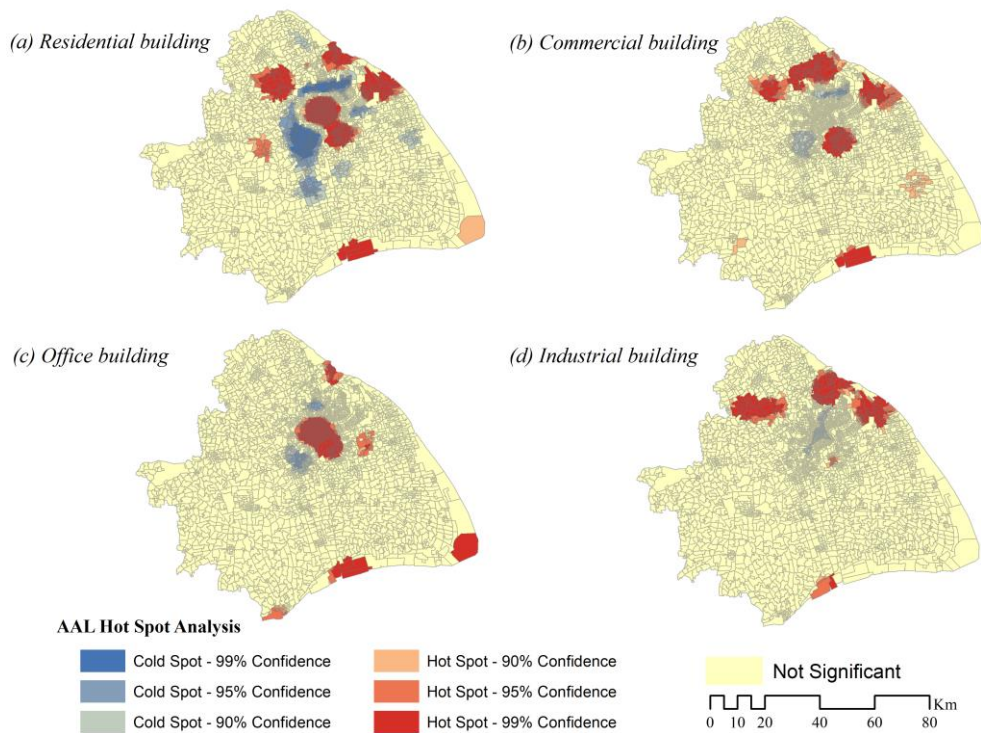
Figure 8. The hot spot analysis of the AAL for buildings at sub-district level in Shanghai.

5 Discussion

5.1 Uncertainties and limitations

270 Our study shows that the damage to buildings in Shanghai grows exponentially with the decreasing likelihood of extreme flood scenarios. For instance, the resulting flood damages to residential, commercial, office, and industrial buildings under the 1/5000-year flooding scenario is more than ten times higher than the resulting damages for a 1/200-year flooding scenario. As shown in section 4.1, the area along the Yangtze River Estuary, Hangzhou Bay, and Huangpu River are broadly flooded under the 1/200, 1/500, 1/1000, and 1/5000-year flooding scenarios. The results of the study show the importance of assessing the

275 risk to extreme events on a regional scale at a high spatial resolution considering the differences in the exposed assets. The hot-spot clusters are distributed over the whole study area and vary from building type to building type. In some areas, the damage is driven mainly by high inundation depths (e.g., the hotspots in the south), whereas other areas face a high risk due to the high vulnerability of the asset values. This emphasizes the importance of assessing the different drivers of risk on the local scale for the selection and dimensioning of adequate protection measures against extreme events.

280 ~~Our assessment of the building damages is comparatively less than those in similar studies of Shanghai. The major reason is that we adopted the construction cost as the values of different buildings, while many other studies calculated the market value of buildings and the associated properties. For instance, Wu et al. (2019) estimated the exposed building asset value in Shanghai to be roughly 304.1 billion USD with a total damage of approximately 32.2 billion USD for a 1/1000-year flood event. Shan et al. (2019) estimated the loss of the residential buildings to be 27.1 billion USD using house price data under a 1/1000-year~~

285 ~~flood event in Shanghai.~~

Apart from our study, there are two other similar flood risk assessments conducted in Shanghai. In the study by Wu et al. (2019), the hazard was defined as a 1/10,000-year fluvial flood scenario (river flood from the Huangpu River) whereas we use several hazard scenarios to cover a broader range of low probability-high impact flood scenarios. For exposure, the building asset value in Shanghai was calculated based on the building floor area, which was obtained from the building floor area per

290 district, and the population density per sub-district. The research estimated the exposed building asset value in Shanghai to be roughly 304.1 billion USD with a total damage of approximately 32.2 billion USD for a 1/10,000-year flood event. In another

11

study by Shan et al. (2019), which focused on the same flood scenarios, damage estimation was determined by considering residential buildings and household properties, using the market price of residential buildings. This research estimated the loss of the residential buildings to be 27.1 billion USD using house price data under a 1/1000-year flood event in Shanghai. It is important to acknowledge that the subject of risk plays a significant role in the risk assessment process. Hazards, exposure, and vulnerability in the context of risk, as described in the latest IPCC report on climate change impacts, may each be subject to uncertainty in terms of magnitude and likelihood of occurrence, and each may change over time and space due to socio-economic changes and human decision-making (IPCC, 2022). Both our study and the previous studies address the three subjects (hazards, exposure, and vulnerability) with extreme flood scenarios, building exposure, and stage-function of buildings. However, due to the different subjects assessed, the resulting risk estimates differ. This disparity observed in the risk assessment conducted in Shanghai can also occur in assessments of other cities.

The integrative analysis of geospatial building asset maps, flood scenarios, and the stage-damage functions in the study makes it possible to assess the flood damage of buildings in the megacity Shanghai with a high spatial resolution. However, the accuracy of building asset values could still be improved. First, the adopted building data of location, footprint area, height and floors didn't consider the construction materials used and years built. Also, the data from 2017 is not very new, considering the fast development of Shanghai. Second, the classification of different types of buildings is quite straightforward based on the land use/land cover data. However, many buildings with multiple functions (e.g., shopping mall and offices) were identified to a single building type, which causes uncertainties of the building value. Third, existing studies' stage-damage functions for specific types of buildings are used to create the asset building damages map for the flood risk assessment. The functions could be updated and tailored to more current and specific building conditions, particularly when estimating flood damages in the future (Ke, 2014). These constraints could be overcome by the inclusion of additional information about age, structures, and utilizations of the buildings. At the end, the methodology of four extreme flood scenarios in Shanghai were taken from published models in Shanghai that are induced by the current physical environment (Wang et al., 2019). However, sea level and heavy precipitation are driven by climate change, so that current flood hazard maps for Shanghai may be outdated in the next few decades. This means that a 1/1000-year event may have a much higher probability in the future and emphasizes the need for proactive adaptation measures. Therefore, climate change scenarios (e.g., sea-level rise, heavy precipitation) should be considered in future flood risk studies. Furthermore, we have access to a rich dataset and extensive research on hazard, exposure, and vulnerability, allowing us to undertake risk analysis chain in Shanghai. This availability of resources can pose a challenge for other cities that may have limited data and research in conducting their own risk assessments.

5.2 Future challenge and adaptation strategies

Future challenge, like extreme flooding events, will become more common in Shanghai. The historical data shows how Shanghai's extreme precipitation events have increased dramatically through time (Wang and Zhou, 2005; Liang and Ding, 2017), which increase the possibility of seawall and levee failures. One 1/1000-year return period flood occurred in Shanghai in 2013, for instance, breaking the highest crest record at Wusongkou Datum and causing levees to breakdown (Ke et al., 2018). Due to climate change, the frequency and/or severity of climate-change related hazards will also increase the flood risks in Shanghai in the future (Woetzel et al., 2020b).

Reviewing these findings from our risk assessment, we highlight the following two points, which in our opinion, might be helpful for advancing the flood risk assessment in the future in Shanghai, or even more broadly in China.

First, the parameters (such as flood hazard maps, damage models, exposure data, etc.) to help perform the flood risk assessment in Shanghai, which are available to the public, are inconsistent and scarce. Flood hazard maps can be an example. Under the current physical environment, coastal flood scenarios with combined effects (sea-level rise, land subsidence, and storm surges) in 2030, 2050, and 2100 that inundate 1.5 %, 37 %, and 50 % of Shanghai, respectively (Wang et al., 2012), have been simulated using a 2D hydrodynamic model (MIKE 21 flow model). On the other hand, fluvial floods from the Huangpu River

shows the different inundation area reaches 0 km^2,111.30 km^2, 124.73 km^2, 143.74km^2, 177.96 km^2, and 195.77 km^2 under

335   1/20, 1/50, 1/100,1/200,1/500, 1/1000-year flood event in Shanghai under the present physical environment (Yin et al., 2013). In our study, the inundation area is 9%, 16%, 24%, and 49% of Shanghai under 1/200, 1/500, 1/1000, and 1/5000-year, respectively. Although we are doing academic research work, it is still important to translate academic findings to everyday language so that inhabitants, stakeholders, and policymakers can improve their capacity for coping with flooding and adapting to it.

340   Second, effective adaptation to increasing flood risks requires an integrated climate response strategy, which shall include a broad scope of intervention measures such as urban planning, structural flood management measures, early warning systems, nature-based solutions, flood awareness and risk financing instruments (Yang et al., 2015; Jongman, 2018; UN, 2020). In table 6, we list potential hard, soft, and hybrid implementation measures and their assumed efficacy in Shanghai. On the other hand, urbanization as a confirmed trend in the fast-developing coastal city may increase asset exposures to floods, but can also offer

345   opportunities for improving flood risk management (Garschagen and Romero-Lankao, 2015). A top-down urban master plan, including land use planning, control of runoff, access to data and information, etc. should be updated, by the Shanghai Municipal Government, to involve advanced risk management measures (Zhou et al., 2017). For instance, in its Master Plan 2017-2035, Shanghai is going to further develop its five new district centers at Jiading, Songjiang, Qinpu (Songjiang-Qingpu low-lying area), Fengxian and Nanhui. These five district centers are planned to be nodal areas in Shanghai and provide more

350   public services for the growing population. However, based on our findings, the Songjiang-Qingpu low-lying area protected by levee with 1/50-year flooding scenario along the Huangpu River, is a hot spot of flood damages. In recognition of this vulnerability, local stakeholders have acknowledged the necessity of implementing levee enhancements in the Songjiang-Qingpu low-lying area. Therefore, future flood protections in these locations, particularly the drainage system and the building structures, must be designed to a higher standard.

355   Table 6. Flood adaptation measures and their potential effecting.

Categories of measures	Specific measures	Effects	Assumed efficacy
Hard measures	Seawall and levees	Protects areas from being flooded or eroded by extreme storms, floods, astronomical tides, and sea-level rise, particularly in low lying areas.	Raise levees and construct a flood barrier in Wusongkou which could lower the flood pressure from Huangpu River (Wang et al., 2011).
	Drainage system	Rapid rainfall discharge to improve transport and safeguard property.	The drainage system should protect Shanghai under 50-year flood scenario. The capacity should be enhanced to the probability period of 100 years in the vulnerability (UPLR, 2018).
	Reservoir	Save part of the precipitation and reduce flood pressure in downstream or lowland areas.	Adjust stock by season or weather forecasting, relieve the pressures of the city flood management during floods.
	Channel	Relieve the flood pressure and speed up drainage within the city.	Ensure that the dam functions could be running on the Huangpu River and Suzhou River.
	Warning system	Enable stakeholders or households to prepare for the extreme climate and react to mitigate it.	Could be used in Shanghai, especially preventing people from putting their lives in extreme flood event.
Soft measures	Dry proofing	Being watertight with all elements substantially impermeable to the entrance of flood and with structural components having the capacity to resist flood loads (FEMA, 2013).	Help the household, especially for households that have experienced regular flooding, to stop the floodwater from their entrance door.
	Wet proofing	Allow water to enter the building but minimizing damage.	Minimizing the damage of property in the building in the flood-prone area.
	Detention and retention areas	Alleviate flood peak by artificially made storage areas (Glavan et al., 2020)	Adapted Sponge City project, to capture, purify and store more water (Griffiths et al., 2020).
	Emergency relief	Personnel evacuation and transfer of property from short-term extreme precipitation.	Adapted in Shanghai, especially residents who lived in inundation areas in the extreme flood scenario.

Insurance	Increase support for people and groups in financial resilience to floods (Surminski and Oramas-Dorta, 2014).	Meet the needs of vulnerable individuals, households and micro, small, and medium-sized enterprises (MSMEs) in Shanghai (Hess and Fischle, 2019).	
Wetlands	Provide valuable flood storage, buffer storm surge, and assist in erosion control (EPA, 2021). Absorb and slow down the floodwater from storm surge.	The wetland on the north of Hangzhou Bay, the mouth of Yangtze River should be protected to slow down the erosion from the storm surge and sea-level rise.	

6 Conclusion

This study presents an integrated impact model of flood damage to buildings based on extreme flooding scenarios in Shanghai. The results show that the inundation area is significantly larger in the low probability-high impact flood scenarios. In all the four considered scenarios, the areas near the Huangpu River and along the coastal areas are always affected with building damages. The central downtown areas of Shanghai have a high risk of being exposed to and affected by extreme floods, partly because of its high building density. Besides that, the Songjiang-Qingpu low-lying area in the west of Shanghai has been recognized as a noticeable area to be flooded under a 1/5000-year flood scenario. This calls for special concerns in the near future because the Songjiang-Qingpu area is planned to become an important sub-center node.

The total asset value for the four building types is 3149 billion USD while the total AAL is 21.9 million dollars. Meanwhile, residential buildings face the highest damage rates of the four types of buildings, accounting for 56 percent of the total AAL, followed by office, industrial, and commercial buildings, respectively. In comparison to other types of buildings, the results show that the residential buildings are significantly vulnerable in all flooding scenarios, which requires attention because residential buildings are a big part of people's daily life.

The presented method offers a possible process to estimate the damage values for residential, commercial, office, and industrial buildings in Shanghai under extreme flooding. The integrated flood model, damage estimation, and risk evaluation are all methodological components that could be implemented to other cities to analyse building damage under extreme flood events. It increases the accuracy and details of flood damage estimates for different types of buildings by considering the direct damage of buildings. The dynamic linkage between the extreme flooding scenarios and the distribution of asset values of the four different types of buildings allows the evaluation of the spatial distribution of flood damages, which would be valuable for individual real estate managers and also for the city government.

Data availability

Data used in this study are available from the first author upon request.

Author Contributions

J.T. analysed the data, conceived, and wrote the paper; J.W. and L.Y. conceived and co-wrote the paper; A.R., M.G. and S.Y. reviewed and improved the analysis and manuscript; M.Z. and L.W. provided the simulation results of the extreme flood scenarios.

References

Arcaids: Construction Cost Handbook 2019 China & Hang Kong, https://www.arcadis.com/en/knowledge-hub/perspectives/asia/research-and-publications/construction-cost-handbook, last access: 20 May 2020.

390 Baidu Maps: https://map.baidu.com/, last access: 15 May 2018.

Balica, S. F., Wright, N. G., and van der Meulen, F.: A flood vulnerability index for coastal cities and its use in assessing climate change impacts, Natural Hazards, 64, 73-105, 10.1007/s11069-012-0234-1, 2012.

C40Cities: Staying Afloat: The Urban Response to Sea Level Rise: https://www.c40.org/other/the-future-we-don-t-want-staying-afloat-the-urban-response-to-sea-level-rise, last access: 14 May 2021.

395 Chan, F. K. S., Yang, L. E., Scheffran, J., Mitchell, G., Adekola, O., Griffiths, J., Chen, Y. B., Li, G., Lu, X. H., Qi, Y. F., Li, L., Zheng, H., and McDonald, A.: Urban flood risks and emerging challenges in a Chinese delta: The case of the Pearl River Delta, Environ. Sci. Policy, 122, 101-115, 10.1016/j.envsci.2021.04.009, 2021.

China Standard Press (CSP): The People's Republic of China Current Land Use Classification (GB/T 21010-2017), 2017.

China Standard Press (CSP): The People's Republic of China Code for Real Estate Appraisal (GB/T 50291-2015), 2015.

400 Chmutina, K., Ganor, T., and Bosher, L.: Role of urban design and planning in disaster risk reduction, Proc. Inst. Civ. Eng.-Urban Des. Plan., 167, 125-135, 10.1680/udap.13.00011, 2014.

Dong, S., Stephenson, W. J., Wakes, S., Chen, Z., and Ge, J.: Mesoscale simulation of typhoon-generated storm surge: Methodology and Shanghai case study, Natural Hazards and Earth System Sciences, 22, 931-945,doi: 10.5194/nhess-22-931-2022, 2022.

405 Du, S. Q., Scussolini, P., Ward, P. J., Zhang, M., Wen, J. H., Wang, L. Y., Koks, E., Diaz-Loaiza, A., Gao, J., Ke, Q., and Aerts, J.: Hard or soft flood adaptation? Advantages of a hybrid strategy for Shanghai, Global Environmental Change, 61, 10, 10.1016/j.gloenvcha.2020.102037, 2020.

Environmental Protection Agency (EPA), https://www.epa.gov/arc-x/climate-adaptation-and-wetland-protection, last access: 10 August 2021.

410 Federal Emergency Management Agency (FEMA), FEMA P-936 ~~Floodfroofing~~ Floodproofing Non-Residential Buildings, 184 pp, 2013.

Garrote, J., Alvarenga, F., and Díez-Herrero, A.: Quantification of flash flood economic risk using ultra-detailed stage–damage functions and 2-D hydraulic models, Journal of hydrology, 541, 611-625, 10.1016/j.jhydrol.2016.02.006, 2016.

Garschagen, M. and Romero-Lankao, P.: Exploring the relationships between urbanization trends and climate change 415 vulnerability, Climatic Change, 133, 37-52, 10.1007/s10584-013-0812-6, 2015.

Glavan, M., Cvejic, R., Zupanc, V., Knapic, M., and Pintar, M.: Agricultural production and flood control dry detention reservoirs: Example from Lower Savinja Valley, Slovenia, Environ. Sci. Policy, 114, 394-402, 10.1016/j.envsci.2020.09.012, 2020.

Gong, S. L. and Yang, S. L.: Effect of Land Subsidence on Urban Flood Prevention Engineering in Shanghai, Scientia 420 Geographic Sinica, 28, 543 - 547, 2008.

Griffiths, J., Chan, F. K. S., Shao, M., Zhu, F. F., and Higgitt, D. L.: Interpretation and application of Sponge City guidelines in China, Philos. Trans. R. Soc. A-Math. Phys. Eng. Sci., 378, 20, 10.1098/rsta.2019.0222, 2020.

Hallegatte, S., Green, C., Nicholls, R. J., and Corfee-Morlot, J.: Future flood losses in major coastal cities, Nature Climate Change, 3, 802-806, 10.1038/nclimate1979, 2013.

425 Hashemi, M. R., Neill, S. P., Robins, P. E., Davies, A. G., and Lewis, M. J.: Effect of waves on the tidal energy resource at a planned tidal stream array, Renewable Energy, 75, 626-639,doi: 10.1016/j.renene.2014.10.029, 2015.

Hess, U. and Fischle, R.: Managing Climate Risk with Extreme Weather Insurance, German Society for International Cooperation, Germany, 6, 2019.

Intergovernmental Panel on Climate Change (IPCC).: Summary for Policymakers, in: IPCC Special Report on the Ocean and
430 Cryosphere in a Changing Climate, Cambridge University Press, Cambridge, UK and New York, NY, USA, 3-36 pp., https://doi.org/10.1017/9781009157964.001, 2019.

Intergovernmental Panel on Climate Change (IPCC).: Point of Departure and Key Concepts in Climate Change 2022: Impacts, Adaptation and Vulnerability, Cambridge University Press, Cambridge, UK and New York, NY, USA, 121-196 pp., doi:10.1017/9781009325844.003, 2022.

435 Jongman, B.: Effective adaptation to rising flood risk, COMMENT, Nature Communications, 9, 3, 10.1038/s41467-018-04396-1, 2018.

Ke, Q.: Flood risk analysis for metropolitan areas–a case study for Shanghai, Hydraulic Engineering, Delft University of Technology, 193 pp., https://doi.org/10.4233/uuid:61986b2d-72de-45e7-8f2a-bd61c725325d, 2014.

Ke, Q., Jonkman, S. N., van Gelder, P., and Bricker, J. D.: Frequency Analysis of Storm-Surge-Induced Flooding for the
440 Huangpu River in Shanghai, China, Journal of Marine Science and Engineering, 6, 17, 10.3390/jmse6020070, 2018.

Kelman, I. and Spence, R.: An overview of flood actions on buildings, Engineering Geology, 73, 297-309, 10.1016/j.enggeo.2004.01.010, 2004.

Liang, P. and Ding, Y. H.: The Long-term Variation of Extreme Heavy Precipitation and Its Link to Urbanization Effects in Shanghai during 1916-2014, Advances in Atmospheric Sciences, 34, 321-334, 10.1007/s00376-016-6120-0, 2017.

445 Manepalli, U. R., Bham, G. H., and Kandada, S.: Evaluation of hotspots identification using kernel density estimation (K) and Getis-Ord (Gi*) on I-630, in: 3rd International Conference on Road Safety and Simulation, Indianapolis Indiana, United States, 14 Sep 2011, 14-16, 2011.

McGrath, H., El Ezz, A. A., and Nastev, M. J. N. H.: Probabilistic depth–damage curves for assessment of flood-induced building losses, 97, 1-14, 10.1007/s11069-019-03622-3, 2019.

450 MIKE: MIKE 21 flow model-hydrodynamic module user guide, 2017.

Nguyen, M. T., Sebesvari, Z., Souvignet, M., Bachofer, F., Braun, A., Garschagen, M., Schinkel, U., Yang, L. E., Nguyen, L. H. K., Hochschild, V., Assmann, A., and Hagenlocher, M.: Understanding and assessing flood risk in Vietnam: Current status, persisting gaps, and future directions, Journal of Flood Risk Management, 14, 24, 10.1111/jfr3.12689, 2021.

Park, K. and Won, J. H.: Analysis on distribution characteristics of building use with risk zone classification based on urban
455 flood risk assessment, International Journal of Disaster Risk Reduction, 38, 10, 10.1016/j.ijdrr.2019.101192, 2019.

Quan, R. S.: Risk assessment of flood disaster in Shanghai based on spatial-temporal characteristics analysis from 251 to 2000, Environmental Earth Sciences, 72, 4627-4638, 10.1007/s12665-014-3360-0, 2014.

Shan, X. M., Wen, J. H., Zhang, M., Wang, L. Y., Ke, Q., Li, W. J., Du, S. Q., Shi, Y., Chen, K., Liao, B. G., Li, X. D., and Xu, H.: Scenario-Based Extreme Flood Risk of Residential Buildings and Household Properties in Shanghai, Sustainability,
460 11, 18, doi: 10.3390/su11113202, 2019.

SMBS: Shanghai Statistical Yearbook-2020, Shanghai: Shanghai MunicpalMunicipal Bureau of Statistics and the National Bureau of Statistics Survey Office in Shanghai, 20212020.

Surminski, S. and Oramas-Dorta, D.: Flood insurance schemes and climate adaptation in developing countries, International Journal of Disaster Risk Reduction, 7, 154-164, 10.1016/j.ijdrr.2013.10.005, 2014.

465 United Nations (UN).: United Nations World Water Development Report 2020: Water and Climate Change, 2020.

UPLR.: SHANGHAI MASTER PLAN 2017-2035, Shanghai Urban Planning and Land Resource Administration Bureau (UPLR), 2018.

Wang, J., Gao, W., Xu, S. Y., and Yu, L. Z.: Evaluation of the combined risk of sea level rise, land subsidence, and storm surges on the coastal areas of Shanghai, China, Climatic Change, 115, 537-558, 10.1007/s10584-012-0468-7, 2012.

470 Wang, J., Xu, S. Y., Ye, M. W., and Huang, J.: The MIKE Model Application to Overtopping Risk Assessment of Seawalls and Levees in Shanghai, International Journal of Disaster Risk Science, 2, 32-42, 10.1007/s13753-011-0018-3, 2011.

Wang, L., Zhang, M., Wen, J., Chong, Z., Ye, Q., and Ke, Q.: Simulation of extreme compound coastal flooding in Shanghai, Advances in water science, 30 (04), 546-555, 2019.

Wang, Y.: Technical Report: Flood damage assessment in Shanghai city. Flood risk map of Shanghai. IWRH. Beijing., 2001.

475 Wang, Y. Q. and Zhou, L.: Observed trends in extreme precipitation events in China during 1961–2001 and the associated changes in large-scale circulation, Geophysical Research Letters, 32, 10.1029/2005GL022574, 2005.

Ward, P. J., de Moel, H., and Aerts, J.: How are flood risk estimates affected by the choice of return-periods?, ?. Natural Hazards and Earth System Sciences, 11, 3181-3195, 10.5194/nhess-11-3181-2011, 2011.

Woetzel, J., Pinner, D., Samandari, H., Engel, H., Krishnan, M., Boland, B., and Cooper, P.: Can coastal cities turn the tide on
480 rising flood risk, McKinsey Global Institute, 2020a.

Woetzel, J., Pinner, D., Samandari, H., Engel, H., Krishnan, M., Boland, B., and Powis, C. J. M. G. I.: Climate risk and response: Physical hazards and socioeconomic impacts, 22, 2020b.

Wu, J. D., Ye, M. Q., Wang, X., and Koks, E.: Building Asset Value Mapping in Support of Flood Risk Assessments: A Case Study of Shanghai, China, Sustainability, 11, 19, 10.3390/su11040971, 2019.

485 Yang, L., Scheffran, J., Qin, H. P., and You, Q. L.: Climate-related flood risks and urban responses in the Pearl River Delta, China, Regional Environmental Change, 15, 379-391, 10.1007/s10113-014-0651-7, 2015.

Yin, J., Yu, D. P., Yin, Z. N., Wang, J., and Xu, S. Y.: Modelling the combined impacts of sea-level rise and land subsidence on storm tides induced flooding of the Huangpu River in Shanghai, China, Climatic Change, 119, 919-932, 10.1007/s10584-013-0749-9, 2013.

490 Yin, J., Yu, D. P., Yin, Z. N., Wang, J., and Xu, S. Y.: Modelling the anthropogenic impacts on fluvial flood risks in a coastal mega-city: A scenario-based case study in Shanghai, China, Landscape and Urban Planning, 136, 144-155, 10.1016/j.landurbplan.2014.12.009, 2015.

Yin, J., Yin, Z. E., Hu, X. M., Xu, S. Y., Wang, J., Li, Z. H., Zhong, H. D., and Gan, F. B.: Multiple scenario analyses forecasting the confounding impacts of sea level rise and tides from storm induced coastal flooding in the city of Shanghai,
495 China, Environmental Earth Sciences, 63, 407-414, 10.1007/s12665-010-0787-9, 2011.

Yu, C., Cheng, X., Hall, J., Evans, E. P., Wang, Y., Hu, C., Wu, H., Wicks, J., Scott, M., and Sun, H.: A GIS-supported impact assessment of the hierarchical flood-defense systems on the plain areas of the Taihu Basin, China, International Journal of Geographical Information Science, 26, 643-665, 2012.

Zhou, Z. Z., Liu, S. G., Zhong, G. H., and Cai, Y.: Flood Disaster and Flood Control Measurements in Shanghai, Natural
500 Hazards Review, 18, 8, 10.1061/(asce)nh.1527-6996.0000213, 2017.